


# Ultrasound-Mediated Gene Delivery Enhances Tendon Allograft Integration in Mini-Pig Ligament Reconstruction

## Journal Article

**Author(s):**

Bez, Maxim; Kremen, Thomas J.; Tawackoli, Wafa; Avalos, Pablo; Sheyn, Dmitriy; Shapiro, Galina; Giaconi, Joseph C.; Ben David, Shiran; [Snedeker, Jess Gerrit](#) ; Gazit, Zulma; Ferrara, Katherine W.; Gazit, Dan; Pelled, Gadi

**Publication date:**

2018-07-05

**Permanent link:**

<https://doi.org/10.3929/ethz-b-000311243>

**Rights / license:**

[Creative Commons Attribution-NonCommercial-NoDerivatives 4.0 International](#)

**Originally published in:**

Molecular Therapy 26(7), <https://doi.org/10.1016/j.ymthe.2018.04.020>

# Ultrasound-Mediated Gene Delivery Enhances Tendon Allograft Integration in Mini-Pig Ligament Reconstruction

Maxim Bez,<sup>1,2</sup> Thomas J. Kremen,<sup>2,3</sup> Wafa Tawackoli,<sup>2,4,5,6</sup> Pablo Avalos,<sup>4</sup> Dmitriy Sheyn,<sup>2,4</sup> Galina Shapiro,<sup>1</sup> Joseph C. Giaconi,<sup>7</sup> Shiran Ben David,<sup>2,4</sup> Jess G. Snedeker,<sup>8</sup> Zulma Gazit,<sup>1,2,3,4</sup> Katherine W. Ferrara,<sup>9</sup> Dan Gazit,<sup>1,2,3,4,5,6</sup> and Gadi Pelled<sup>1,2,4,5,6</sup>

<sup>1</sup>Skeletal Biotech Laboratory, The Hebrew University-Hadassah Faculty of Dental Medicine, Ein Kerem, Jerusalem 91120, Israel; <sup>2</sup>Department of Surgery, Cedars-Sinai Medical Center, Los Angeles, CA 90048, USA; <sup>3</sup>Department of Orthopedics, Cedars-Sinai Medical Center, Los Angeles, CA 90048, USA; <sup>4</sup>Board of Governors Regenerative Medicine Institute, Cedars-Sinai Medical Center, Los Angeles, CA 90048, USA; <sup>5</sup>Biomedical Imaging Research Institute, Cedars-Sinai Medical Center, Los Angeles, CA 90048, USA; <sup>6</sup>Department of Biomedical Sciences, Cedars-Sinai Medical Center, Los Angeles, CA 90048, USA; <sup>7</sup>Department of Imaging, Cedars-Sinai Medical Center, Los Angeles, CA 90048, USA; <sup>8</sup>Department of Orthopedics, University of Zurich, Zurich 8008, Switzerland; <sup>9</sup>Department of Biomedical Engineering, University of California, Davis, Davis, CA 95616, USA

**Ligament injuries occur frequently, substantially hindering routine daily activities and sports participation in patients. Surgical reconstruction using autogenous or allogeneic tissues is the gold standard treatment for ligament injuries. Although surgeons routinely perform ligament reconstructions, the integrity of these reconstructions largely depends on adequate biological healing of the interface between the ligament graft and the bone. We hypothesized that localized ultrasound-mediated, microbubble-enhanced therapeutic gene delivery to endogenous stem cells would lead to significantly improved ligament graft integration. To test this hypothesis, an anterior cruciate ligament reconstruction procedure was performed in Yucatan mini-pigs. A collagen scaffold was implanted in the reconstruction sites to facilitate recruitment of endogenous mesenchymal stem cells. Ultrasound-mediated reporter gene delivery successfully transfected 40% of cells recruited to the reconstruction sites. When *BMP-6* encoding DNA was delivered, *BMP-6* expression in the reconstruction sites was significantly enhanced. Micro-computed tomography and biomechanical analyses showed that ultrasound-mediated *BMP-6* gene delivery led to significantly enhanced osteointegration in all animals 8 weeks after surgery. Collectively, these findings demonstrate that ultrasound-mediated gene delivery to endogenous mesenchymal progenitor cells can effectively improve ligament reconstruction in large animals, thereby addressing a major unmet orthopedic need and offering new possibilities for translation to the clinical setting.**

## INTRODUCTION

Ligament injuries are commonly encountered in orthopedic clinical practice; they account for substantial patient morbidity, particularly in the young active population.<sup>1,2</sup> The anterior cruciate ligament (ACL) of the knee is one of the most commonly injured soft-tissue

structures. Approximately 100,000 ACL reconstructions are performed in the United States each year.<sup>3,4</sup> ACL reconstruction requires the implantation of autologous or allogeneic tissue into bone tunnels drilled in the tibia and femur. These procedures are associated with a prolonged period of rehabilitation,<sup>3</sup> persistent knee instability, and abnormal functional outcomes.<sup>5</sup> In one study, only 63% of patients who received ACL reconstruction returned to their pre-injury level of sports participation and 44% were able to return to competitive sports.<sup>6</sup> In addition, up to 25% of patients undergoing ACL reconstruction suffer secondary injuries within 2 years of returning to sports.<sup>7</sup> These outcomes are especially devastating because some of these patients are young and physically active and must face long-term disability, repeated surgeries, loss of working days, and considerable health care costs.

Successful soft-tissue graft reconstruction requires adequate and timely graft integration at the ligament-bone interface. An accelerated healing process could reduce the risk of graft failure and enable faster return of patients to physical activity.<sup>8</sup> However, the early healing process is believed to be hampered by loose bone-graft attachment and hypoxic conditions at the attachment site.<sup>9</sup> This may lead to tunnel widening and increased graft laxity, limiting patients' rehabilitation and return to activity.<sup>10</sup> Currently, knee ligament reconstructions are performed using either autogenous or allogeneic tissues. These grafts can be composed of soft tissue or a composite of soft tissue and bone. Soft-tissue grafts are the most commonly utilized graft source in the United States as well as worldwide, with up to 79% of patients undergoing ACL reconstruction receiving hamstring tendon

Received 25 November 2017; accepted 20 April 2018;  
<https://doi.org/10.1016/j.ymthe.2018.04.020>

**Correspondence:** Gadi Pelled, Department of Surgery, Cedars-Sinai Medical Center, 8700 Beverly Boulevard, Los Angeles, CA 90048, USA.

**E-mail:** [gadi.pelled@cshs.org](mailto:gadi.pelled@cshs.org)

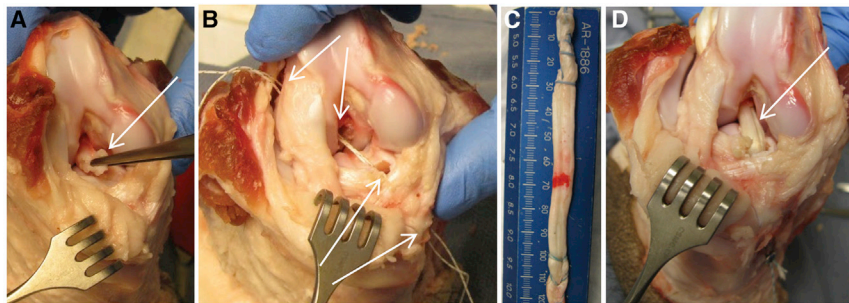


**Figure 1. ACL Reconstruction Model in Yucatan Mini-Pig Knee Joints**

(A) During surgery, the ACL is transected at its tibial and femoral attachments and excised (denoted by arrow). (B) The tibial and femoral tunnels are drilled (arrows), and the required graft length is assessed. (C) The allograft is truncated to the appropriate length and prepared using a running lock suture at each terminus. (D) The allograft (arrow) is inserted into the drilled bone tunnels and tied using sutures to anchor it to cortical screws.

grafts.<sup>11–14</sup> Integration of allograft ACL reconstructions takes longer than that of autograft reconstructions;<sup>15,16</sup> however, autograft harvesting is associated with higher rates of morbidity, which negatively impacts postoperative rehabilitation<sup>17</sup> and makes autograft reconstruction less appealing for clinical use. Considering this, the development of new therapeutic interventions with the ability to enhance and accelerate allograft osteointegration would have a tremendous clinical impact.

Several biological approaches have been proposed to enhance ligament-bone integration.<sup>4</sup> These strategies include delivery of osteoinductive growth factors or platelet-rich plasma, viral transduction of genes encoding bone morphogenetic protein (BMP) or cyclo-oxygenase 2, and cell-based therapies.<sup>3</sup> However, growth factors need to be injected repeatedly due to their short half-lives and can be very expensive. Viral vectors may be immunogenic and tumorigenic, and implantable cell therapies require complex *ex vivo* manipulation and would likely necessitate a prolonged regulatory and approval process. These disadvantages would likely prevent the widespread clinical translation of these therapeutic approaches.

An attractive alternative would be nonviral delivery of osteogenic genes to the site of the graft-bone junction. Although viral vectors are considered more efficient for gene delivery than most nonviral methods, the efficiency of *in vivo* nonviral gene delivery can be enhanced using a short pulse of energy.<sup>18</sup> Such a method induces formation of transient nano-sized pores in the membranes of cells, enabling improved DNA uptake and subsequent transgene expression. We previously showed that targeted ultrasound-mediated gene delivery could be successfully used to transduce endogenous progenitor cells using a two-step procedure. We first implanted a biodegradable scaffold to recruit endogenous stem cells and then used microbubble-enhanced DNA sonoporation to deliver the *BMP* gene to the recruited cells. When *BMP-6* gene was used, the treatment resulted in complete regeneration of critical-size tibia bone fractures in a mini-pig model.<sup>19</sup> In the present study, we hypothesized that microbubble-enhanced, ultrasound-mediated gene delivery of a *BMP* gene would lead to enhanced integration of an implanted ACL graft in a clinically relevant, large-animal (porcine) model. Multiple molecular, structural, and biomechanical parameters were used to demonstrate the feasibility of this therapeutic approach.

## RESULTS

### Sonoporation Leads to Reporter Gene Expression in Endogenous Progenitors Recruited to ACL Reconstruction Sites

Six mini-pigs underwent surgery, during which each animal's native ACL was resected and an allograft was implanted into drilled tibial and femoral bone tunnels (Figure 1). A collagen scaffold was implanted at the two ends of the allograft tissue within the bone tunnels. The bone tunnels were treated with microbubble-enhanced ultrasound-mediated gene delivery 14 days after surgery. Plasmid DNA encoding GFP, mixed in microbubbles, was transcutaneously injected into the reconstruction site in all animals, whereas half of the animals were randomly allocated to subsequent treatment with ultrasound (Figure 2). Flow cytometry, performed on day 19 post-scaffold implantation, revealed that approximately 15% of cells collected from within the reconstruction drill sites were positive for mesenchymal stem cell (MSC) markers CD29, CD44, and CD90 (Figure 3).

Next, the efficacy of ultrasound-mediated gene delivery was assessed. Flow cytometry analysis performed on day 5 post-transgene delivery showed that 45% of isolated cells from the reconstruction sites were GFP positive in animals treated with ultrasound ("US" group), three times more than observed in untreated animals ("no US" group;  $p < 0.05$ ; Figure 4A). GFP-expressing cells from reconstruction sites in ultrasound-treated animals were also twice as fluorescent as cells from reconstruction sites in animals not subjected to ultrasound ( $p < 0.05$ ; Figure 4B). Interestingly, among transfected cells in the ultrasound-treated group, significantly more cells expressed the MSC markers CD29, CD44, and CD90. An examination of GFP-positive cells in the ultrasound-treated group demonstrated that 15% were CD29 positive, 25% were CD44 positive, and 10% were CD90 positive, whereas in the untreated group, only 1% of GFP-positive cells were CD29 positive, 7% were CD44 positive, and 3% were CD90 positive ( $p < 0.05$ ; Figures 4C–4E). Overall, ultrasound-treated reconstruction sites exhibited significantly higher progenitor transfection rates as well as stronger transgene expression levels.

### Sonoporation Induces BMP-6 Expression at Reconstruction Sites and Enhances Osteointegration

Six animals underwent ACL surgery as described above and were treated with either ultrasound-mediated delivery of *BMP-6* plasmid and microbubbles ("BMP-6 + US" group) or injection of *BMP-6*

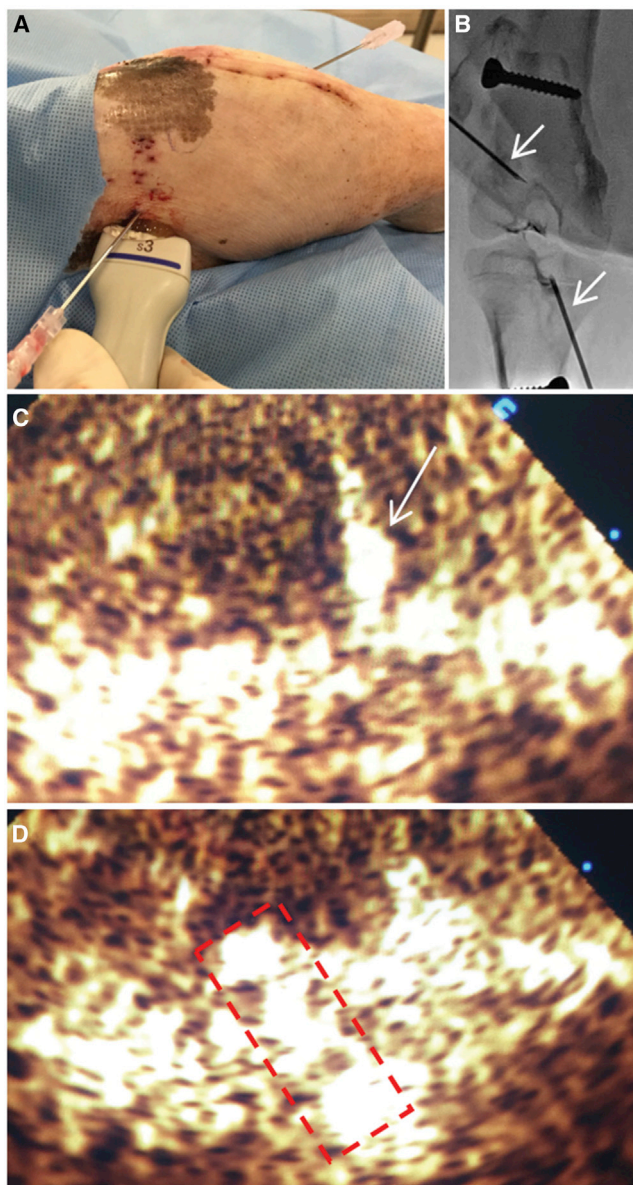


**Figure 2. Ultrasound Treatment Setup**

(A) Injection of a DNA and microbubble mixture into the bone tunnel sites. The ultrasound probe is placed adjacent to the needle for optimal visualization of the injected mixture. (B) Fluoroscopic imaging of needle placement within the bone tunnel sites is shown. Arrows denote the inserted needles. (C) Ultrasound contrast agent imaging during injection of the plasmid and microbubbles mixture is shown. Arrow denotes the inserted needle in the tunnel. (D) Ultrasonographic visualization of the injected mixture (marked with dashed line) within the bone tunnel during sonoporation is shown.

plasmid and microbubbles without ultrasound application (“BMP-6” control group). Local expression of the *BMP-6* gene following sonoporation directed to reconstruction sites was evaluated 5 days after gene delivery. qPCR analysis performed on cells isolated from the reconstruction bone tunnels showed 15-fold higher *BMP-6* expres-

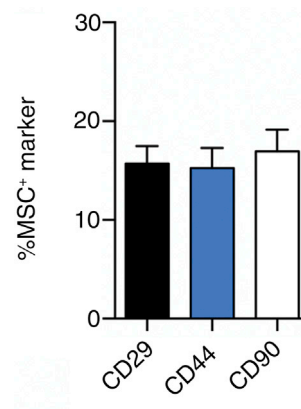


**Figure 3. Recruitment of Endogenous Mesenchymal Progenitor Cells to ACL Bone Tunnels**

Flow cytometry analysis of CD29-, CD44-, and CD90-positive cells from bone tunnel sites 19 days postoperatively (MSC, mesenchymal stem cell). Data are represented as mean  $\pm$  SEM.

sion in ultrasound-treated animals compared to control animals ( $p < 0.01$ ; Figure 5A). Next, the therapeutic effect of local *BMP-6* gene delivery was evaluated. Ten animals underwent surgery as described above. Osteointegration in animals treated with *BMP-6* and ultrasound (*BMP-6* + US group) was compared to osteointegration in animals treated with *BMP-6* plasmid without ultrasound (*BMP-6* group). Micro-computed tomography ( $\mu$ CT) analysis performed 8 weeks after surgery revealed that reconstruction sites treated with *BMP-6* DNA and ultrasound contained twice the bone volume observed in sites in control animals ( $p < 0.01$ ; Figures 5B–5D), but no ectopic bone formation was observed in any of the treated animals (Figure 5E). Histological evaluation of the treated animals revealed tissue continuity with the formation of perpendicular collagen fibers and direct bone insertions between the graft and the osseous tunnel (Figure 5F). In contrast, in the control animals, there was a well-demarcated border between the graft and the osseous tunnel, which was filled with poorly organized granulation tissue without continuity between the graft and the adjacent bone. No mononucleated cells infiltrated the grafts, suggesting an absence of inflammatory reaction to the therapy.

### **BMP-6 Gene Delivery Induces Rapid Functional Healing of Treated Knee Joints**

Anteroposterior (AP) knee laxity and tensile failure testing were performed on treated animals' knees to examine their mechanical properties 8 weeks after surgery. In accordance with the  $\mu$ CT results, AP laxity measured at  $\pm 20$  N in the *BMP-6* + US group was 2-fold lower than that in control animals, demonstrating superior knee joint stability ( $p < 0.05$ ; Figure 6A). In addition, knees in animals treated with *BMP-6* and ultrasound had approximately three times higher linear stiffness and maximum load to failure, showing stronger graft-bone integration than that found in control animals ( $p < 0.05$ ; Figures 6B and 6C).



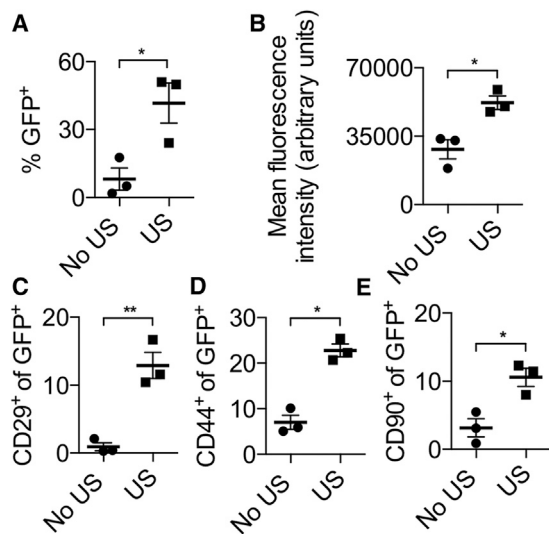


**Figure 4. Reporter Gene Expression in Mini-pig Reconstruction Sites following Ultrasound-Mediated Gene Delivery**

(A) Flow cytometry analysis of the percentage of GFP-positive cells isolated from bone tunnel sites, with or without ultrasound treatment, 5 days after treatment. (B) Mean fluorescence intensity per cell in GFP-positive cells isolated from bone tunnels is shown. (C–E) Percentage of GFP-positive cells positive for CD29 (C), CD44 (D), and CD90 (E).  $n = 3$  per experimental group; \* $p < 0.05$ ; \*\* $p < 0.01$ ; no US, group in which no ultrasound was used; US, group in which ultrasound was used. Data are represented as mean  $\pm$  SEM.

## DISCUSSION

In this study, we used ultrasound-mediated, microbubble-enhanced gene delivery to improve *in situ* ACL graft osteointegration in a mini-pig model. We showed that ultrasound-mediated *BMP-6* DNA delivery to cells residing within the reconstruction site achieved local gene expression, targeting endogenous MSCs. Osteogenic gene delivery resulted in enhanced allograft integration and tunnel narrowing, with significantly superior biomechanical properties of the reconstructed ACLs as soon as 8 weeks after the surgery. Importantly, no evidence of ectopic bone formation or inflammatory response was observed, suggesting a favorable safety profile. Using a sonographic system set at parameters used in the clinical setting, we saw no clinical or histological signs of heating or heat-associated damage.

Currently, surgical treatment of musculoskeletal soft-tissue injuries includes ligament reconstructions and primary repairs. Although successful ligament-to-bone healing is critical to restore function and stability to the injured joint,<sup>20</sup> current treatment strategies lead mostly to fibrotic scar formation. It is this fibrosis that probably results in limited mechanical stability at the soft tissue-bone junction site and a lack of functional integration, causing graft failure.<sup>3,21</sup> This is particularly true in the early phases of graft healing, as demonstrated by gradual increases in instrumented knee laxity following ACL reconstruction.<sup>22</sup> The reconstructed graft may elongate due to delayed osteointegration, leading to excessive laxity and relative knee instability.<sup>23,24</sup> Because our approach leads to accelerated osteointegration with reduced AP

laxities, it may lessen graft elongation and achieve better knee stability after surgery.

Bone tunnel widening has been reported to occur in up to 40% of ACL reconstructions.<sup>25–27</sup> Tunnel widening has been observed with use of all graft types, including autograft bone-patellar tendon-bone grafts.<sup>26,28,29</sup> It represents a significant geographic deficiency of bone at the ACL attachment sites and may delay proper formation of the enthesis.<sup>26,30,31</sup> It may delay graft integration or lead to graft failure in the short term and may complicate long-term management if revision ACL reconstruction procedures are necessary. Tunnel widening may require an additional separate bone grafting procedure to regenerate bone within the tunnel before a revision may be possible. Therefore, our approach is especially attractive because it does not cause tunnel widening and, instead, rapidly increases bone formation at the graft-bone integration site.

Several groups have used *BMP* gene delivery to enhance integration of ACL grafts. Martinek et al.<sup>32</sup> delivered a viral vector encoding *BMP-2* to the graft-bone interface in rabbits by infecting the graft *in vitro* prior to implantation. Those researchers found increased bone formation at the graft-bone interface with superior biomechanical properties at 8 weeks after treatment. Wang et al.<sup>33</sup> implanted cells infected with adenovirus-*BMP-2* into a graft-bone interface in rabbits, showing biomechanical superiority at 12 weeks after implantation.<sup>34</sup> We have previously shown that *BMP-6*-transfected MSCs led to significantly enhanced osteogenic differentiation and bone formation compared to *BMP-2*, both *in vitro* and *in vivo*.<sup>35</sup> These differences can be attributed to previous evidence showing that these proteins work through different signal transduction pathways.<sup>36–38</sup> To the best of our knowledge, our present study is the first work to show that a nonviral gene delivery approach can achieve increased graft osteointegration and improved biomechanical properties as soon as 8 weeks after surgery in a large-animal model, which better represents human anatomy and biology. Because *BMP-6*-engineered MSCs exert a dual autocrine-paracrine response when used for tissue engineering, it is beneficial to target the residing MSCs and bone progenitor cells within the reconstruction site to achieve a greater effect.<sup>39,40</sup> Compared to previous works, our approach does not require cell isolation or *in vitro* processing, making it more feasible for future clinical applications in humans.

In this study, we used a two-step procedure that included recruitment of endogenous progenitor cells to the reconstruction site. We showed that, by implanting a collagen scaffold in the reconstruction site, efficient endogenous progenitor migration and retention in the scaffold could be achieved within 19 days, resulting in a viable cell population for gene delivery and avoiding the need for *ex vivo* cell manipulation. We were able to demonstrate that 20%–30% of the transfected cells were also positive for MSC surface markers. Moreover, we showed that this approach led to localized transgene expression and did not lead to ectopic bone formation. We previously showed that this delayed approach resulted in transient gene expression lasting for 10 days and complete regeneration of critical-size fractures in

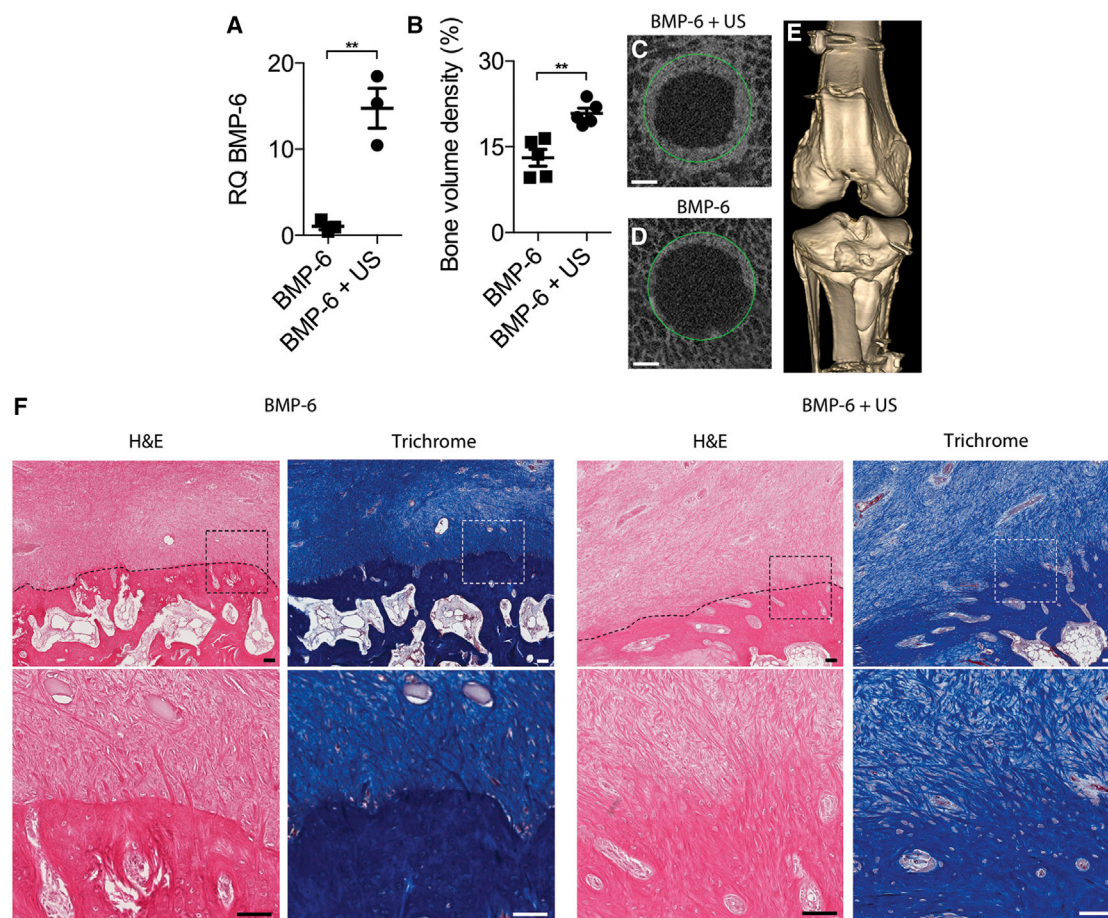


**Figure 5. Ultrasound-Mediated *BMP-6* Gene Delivery to Mini-pig ACL Reconstruction Sites**

(A) *BMP-6* gene (relative quantification [RQ]) expression in bone tunnels at ACL reconstruction sites 5 days after treatment. (B) Quantitative analysis of bone formation in reconstruction sites 8 weeks after surgery is shown. (C and D) Representative  $\mu$ CT slices of bone tunnels that received (C) or did not receive (D) ultrasound treatment, obtained 8 weeks after surgery, are shown. Green circles denote the original diameters of the bone tunnels created during surgery. The scale bars represent 1 mm. (E) Fluoroscopic 3D reconstruction of a representative *BMP-6* and ultrasound-treated knee joint is shown. (F) Masson's trichrome and H&E staining of the bone-graft interface 8 weeks after surgery at low magnification (upper) and at high magnification of tissue in the marked squares (lower) is shown. Dotted lines show boundaries between grafts and calcified tissues. The scale bars represent 100  $\mu$ m.  $n = 3$  per experimental group in the gene expression study;  $n = 5$  per experimental group in the bone formation study; \*\* $p < 0.01$ . Data are represented as mean  $\pm$  SEM.

mini-pigs.<sup>19</sup> Whereas in the current study we did not compare this approach to non-delayed gene delivery using sonoporation, we believe that allowing cell recruitment may well compensate for the lower transfection efficacy of local nonviral gene delivery approaches. Due to technical limitations resulting in lower amount of extracted tissue from the sonoporated sites, we could not properly assess the amount of secreted BMP-6.

The study described here provides an initial proof of concept that should be followed by further experiments exploring the potential of the method. We did not compare the use of sonoporation to the use of collagen scaffold alone, because previous studies in a similar pig model have shown that the addition of a collagen scaffold to the graft did not result in improved healing.<sup>41</sup> Our hypothesis was

that the expression of the BMP gene would drive the osteointegration of the ACL graft to bone. Hence, we did not include a group of animals treated with ultrasound-mediated gene delivery of an empty plasmid that would not induce BMP overexpression.

Another interesting aspect of the proposed method is the use of repeated treatments. As this therapy can be easily and minimally invasively repeated, multiple treatments may be used to further enhance osteointegration and promote faster and improved healing. However, prolonged ultrasound exposure could result in a variety of adverse effects, including excessive tissue heating and dystrophic calcifications due to tissue damage.<sup>42</sup> Efficacy and safety still need to be considered. In addition, further studies are needed to compare this approach to the use of autologous grafts, which are currently more utilized in

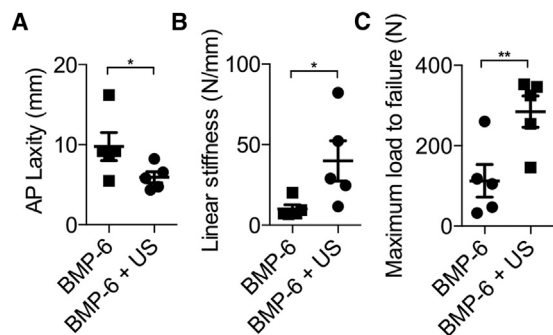


**Figure 6. Biomechanical Properties of Knee Joints following Ultrasound-Mediated Gene Delivery**

(A) AP laxity testing of ultrasound-treated and untreated knee joints. (B and C) Linear stiffness (B) and maximum load to failure (C) in implanted grafts at the ACL reconstruction site during tensile failure testing 8 weeks after treatment are shown. AP, anteroposterior; N, Newton;  $n = 5$  per experimental group; \* $p < 0.05$ ; \*\* $p < 0.01$ . Data are represented as mean  $\pm$  SEM.

the clinical setting due to improved osteointegration and other control groups as indicated above. Based on our results so far, it is feasible that combining the ultrasound-mediated *BMP* gene delivery approach to an autograft would further enhance and accelerate ACL reconstruction.

These results indicate great promise for future ultrasound-mediated gene therapies for tissue regeneration. Because ultrasound technology is safe and widely used in the clinic, this approach can be easily translated into clinical practice. The introduction of microbubbles, which are also a US Food and Drug Administration (FDA)-approved ultrasound contrast agent, allows localization of injected material and real-time monitoring of the sonoporation procedure at the treatment site. This method has the potential to be used for many different applications based on *in situ* tissue engineering. In the context of tendon and ligament injuries, this therapy can be applied to a variety of orthopedic indications to enhance ligament-to-bone healing. It is minimally invasive and does not require *ex vivo* stem cell manipulation, harvest of the patient's own tissue, or use of costly growth factors. In summary, ultrasound-mediated gene therapy is a promising tool that may offer a positive response to a wide variety of patients suffering from soft-tissue musculoskeletal injuries.

## MATERIALS AND METHODS

### Study Design

The objective of our study was to enhance ACL allograft integration using ultrasound-mediated endogenous MSC engineering. We hypothesized that ultrasound-mediated, microbubble-enhanced gene delivery of the *BMP-6* gene would lead to accelerated graft integration in a clinically relevant large-animal model. Male and female Yucatan mini-pigs (S&S Farms) were used in this study. The mean weight  $\pm$  SD of the animals was  $37.0 \pm 3.6$  kg, and their mean age  $\pm$  SD was  $7.8 \pm 1.2$  months. The sample size used was estimated to achieve a power of 0.8 and  $\alpha = 0.05$  using one-way ANOVA.

Sonoporation was investigated for its capacity to enhance integration of an implanted ACL graft in a reconstruction site. Mini-pigs underwent surgery in which the native ACL was transected. Next, tendon allografts were implanted in tunnels created in the femoral and tibial bones and anchored to cortical screws placed approximately 1 cm from the bone tunnel apertures. In addition, collagen scaffolds were implanted within the bone tunnels. Fourteen days later, the pigs were randomly assigned to (1) a treatment group, in which they received *BMP-6* plasmid premixed with microbubbles, which was injected into the reconstruction site followed by ultrasound application (*BMP-6 + US* group) or (2) a control group, in which the animals received an injection of *BMP-6* plasmid premixed with microbubbles without ultrasound application. Control groups in which only a collagen scaffold was implanted (no gene delivery) or an ultrasound mediated delivery of an empty plasmid was used instead of *BMP-6* were not included in this study, as we have shown that such treatments did not result in any significant biological effect.<sup>19</sup> Sonoporation efficiency was determined using flow cytometry for reporter gene expression and qRT-PCR for *BMP-6* gene expression. Bone formation and graft integration were assessed using  $\mu$ CT, histology, and biomechanical testing.

### Plasmid DNA Production

A plasmid encoding EGFP under the control of the cytomegalovirus promoter (*pCMV-EGFP-N1*) was used to study transgene expression. A plasmid encoding human *BMP-6* under the control of the cytomegalovirus promoter (*pCMV-BMP6*) was used to induce entheses. Plasmid preparation is detailed elsewhere.<sup>35,43</sup> All plasmids were expanded using standard laboratory procedures and purified using an EndoFree Kit (QIAGEN, Valencia, CA).

### Allograft Preparation

Porcine flexor tendon allografts were harvested from mini-pigs post mortem by using an aseptic technique described by Hirpara et al.<sup>44</sup> Harvested tendons were placed immediately into a sterile plastic bag, and their surfaces were swabbed with a culture swab. The allografts and culture swab tubes were then sent to Veterinary Transplant Services (Kent, WA) for standard allograft processing, including freezing and bacteriological testing.

### ACL Reconstruction: Animal Model

All animal procedures were approved by the Cedars-Sinai Medical Center Institutional Animal Care and Use Committee (IACUC #00614). Animals were fasted for approximately 18 hr before the surgical procedure. Each mini-pig was sedated with intramuscular (IM) acepromazine (0.25 mg/kg, IM), ketamine (20 mg/kg, IM), and atropine (0.02–0.05 mg/kg, IM) followed by propofol (2 mg/kg, intravenous [i.v.]). Animals were intubated, and anesthesia was maintained using 1.0%–3.5% inhaled isoflurane for the duration of the surgical procedure. The animals were kept warm during the surgical procedure by using a Bair Hugger (3M, Maplewood, MN) to prevent unintended hypothermia.

An open midline approach was used for each animal's right knee followed by a medial parapatellar arthrotomy. The ACL was transected at



its tibial and femoral attachments and excised (Figure 1A). Using a RetroConstruction Drill Guide (Arthrex, Naples, FL), a 2.4-mm drill-guide pin was drilled into the joint from the anteromedial proximal tibia to the anatomical tibial footprint of the native ACL. A 7-mm cannulated drill was used over the drill-guide pin to construct the tibial tunnel, utilizing an outside-in technique and taking care not to injure the intra-articular structures. The femoral tunnel was constructed in a similar outside-in fashion using the drill-guide pin, which was centered at the femoral footprint of the native ACL (Figure 1B). Two cortical screw anchors were inserted: one approximately 1 cm proximal to the femoral tunnel and the other approximately 1 cm distal to the tibial tunnel, in line with the trajectory of the tunnels.

We assessed the total projected maximal graft length, consisting of the sum of the femoral tunnel length, tibial tunnel length, and intra-articular distance between the two tunnels with the knee placed in extension. The allograft tendons were thawed and truncated to the appropriate length, which was 1 cm less than the projected maximal graft length (Figure 1C). The allograft was prepared using a no. 2 FiberLoop (Arthrex, Naples, FL), in a running lock fashion for reinforcement, at each terminus and then shuttled in the femoral and tibial tunnels. A flat sheet of biodegradable collagen scaffold (DuraGen Plus, Integra LifeSciences) with a 100- $\mu$ m pore size was then wrapped circumferentially around each graft terminus and fashioned so that approximately 5 mm of the collagen scaffold outside the central allograft core occupied the superficial portion of the femoral and tibial tunnel extra-articular apertures.

After positioning the allograft and collagen scaffold construct within the bone tunnels, the graft was tied over the femoral cortical screw post and tensioned by using manual traction for several minutes to remove any graft creep (Figure 1D). After cycling the knee through a range of flexion and extension for approximately 10 times, the tibial terminus of the graft was secured over the tibial cortical screw post, with the knee in near full extension and a posterior drawer force held on the tibia. The surgical site was closed in layers, and a sterile dressing was applied.

#### Ultrasound-Mediated, Microbubble-Enhanced Gene Delivery

Fourteen days after surgery, the animals were sedated in the manner described above. First, a microbubble suspension (Definity, Lantheus Medical Imaging, N. Billerica, MA) was activated by 45 s of shaking using a Vialmix shaker (Lantheus Medical, N. Billerica, MA). Then,  $5 \times 10^6$  microbubbles and 0.5 mg plasmid DNA were mixed together in a total volume of 0.5 mL. To avoid microbubble aggregation and adhesion to the syringe walls, the syringe containing the mixture was manually rotated periodically prior to injection. Next, the tunnels were located using a fluoroscan mini C-arm (Hologic, Bedford, MA), and an 18G needle was inserted into the center of each tunnel (Figures 2A and 2B). The mixture was injected while being visualized using a Sonos 5500 unit (Philips Ultrasound, Andover, MA) equipped with a focused S3 probe that had been set to B-mode with its focal point matching the location of the tunnel. Then, a therapeutic ultrasonic pulse was applied using the contrast agent imaging mode at a

transmission frequency of 1.3 MHz, a mechanical index of 1.2, and a depth of 3 cm for approximately 2 min until the microbubbles were no longer visible (Figures 2C and 2D).

#### Transfection Efficacy Evaluation: GFP Expression

Six animals underwent surgery as described above. Fourteen days later, the mini-pigs were injected with GFP plasmid premixed with microbubbles. The animals were randomly assigned so that half were treated with ultrasound immediately after the injection. Five days post-transfection, the animals were sacrificed. Post mortem, tissue was extracted from both bone tunnels, washed with PBS, digested using 0.1% collagenase (type 1A; Sigma-Aldrich, St. Louis, MO) for 1 hr, filtrated using a 70  $\mu$ m cell strainer, and centrifuged at 2,000 rpm for 7 min. The freshly harvested cells were analyzed for GFP expression by using an LSR-II flow cytometer, BD FACSDiva, and FCS Express software (BD Biosciences, Heidelberg, Germany). The percentage of GFP-positive cells was used to estimate the transfection rate. We also characterized the surface markers of transfected cells (taking into consideration the limited availability of anti-pig antibodies). Cells were stained with mouse anti-human (with cross-reactivity to pig) CD90, mouse anti-pig CD29 (BD Pharmingen, San Diego, CA), and rat anti-pig CD44 (Fitzgerald Industries International, Acton, MA, USA). Primary antibodies were detected by applying the fluorochrome-conjugated secondary antibodies rat anti-mouse-phycoerythrin (PE) (BD Pharmingen) and donkey anti-rat-PE (Imgenex, San Diego, CA) according to the manufacturers' recommendations.

#### BMP-6 Gene Expression Analysis

Six animals underwent surgery and 14 days postoperatively were injected with BMP-6 plasmid premixed with microbubbles. The animals were randomly assigned so that half were treated with ultrasound immediately after the injection. The animals were sacrificed 5 days after ultrasound-mediated gene transfection. Tissues were collected post mortem to characterize BMP-6 gene expression, and RNA was isolated using an RNeasy extraction kit (Qiagen, Hilden, Germany). qRT-PCR was done to estimate BMP-6 gene expression using the ABI7500 Prism system (Applied Biosystems, Foster City, CA) with Hs00233470\_m1 primer (ABI). 18 s was used as a housekeeping gene control.

#### Bone Tunnel Narrowing Analysis Using $\mu$ CT

Twelve mini-pigs underwent surgery and were injected with BMP-6 plasmid premixed with microbubbles. The animals were randomly assigned so that half were treated with ultrasound immediately after the injection. Eight weeks postoperatively, the animals were euthanized and the operated knees were harvested for *ex vivo* high-resolution  $\mu$ CT (vivaCT 40; Scanco Medical AG, Brüttisellen, Switzerland), as previously described.<sup>45</sup> Microtomographic slices were acquired using an X-ray tube with a 55 kVp potential and reconstructed at a voxel size of 35  $\mu$ m. The bone tunnels were evaluated using histomorphometric 3D evaluation. A constrained 3D Gaussian filter ( $\sigma = 0.8$ ; support = 1) was used to partly suppress noise in the volume of interest. The bone tissue was segmented from marrow and soft tissue by using a global thresholding procedure. A quantitative assessment of



bone volume density and apparent density, based on microtomographic datasets, was created using direct 3D morphometry.

### Histological Evaluation

One specimen from each treatment group was used for histological evaluation, as previously described.<sup>46,47</sup> Briefly, the bone samples were fixed in 4% formalin, decalcified, and embedded in paraffin. Tissue sections were cut at a thickness of 5  $\mu\text{m}$  and subsequently stained using H&E. The slides were imaged using Aperio ScanScope AT Turbo (Leica Biosystems, Wetzlar, Germany) with 20 $\times$  magnification. All samples were scanned using the same gain and exposure settings.

### Biomechanical Analysis

Five knee joints from each group were used for biomechanical analysis, as previously described.<sup>48,49</sup> Following tissue harvest, eight weeks post-surgery, the knee joints were wrapped in normal saline-soaked gauze, sealed, and frozen until analysis. Prior to the analysis, the samples were thawed for approximately 24 hr at room temperature. Soft tissue was carefully removed from the joint, leaving the knee capsule intact. Specimens were kept moist throughout the test protocol by wrapping them in a normal saline-soaked gauze.

Cyclic AP laxity testing was performed with the knee flexed at 60°. The knees were supported on custom-made fixtures and rigidly attached to a universal testing machine (Zwick 1456; Zwick, Ulm, Germany). For AP laxity testing, fully reversed sinusoidal AP-directed shear loads of  $\pm 20$  N were applied at 0.0833 Hz for 12 cycles. The first three cycles were performed to precondition the joint, and the laxity values for the remaining cycles were averaged. Load and displacement data were acquired and plotted to obtain the load-displacement curve. During the AP laxity tests, axial rotation was locked in the neutral position, whereas the varus-valgus angulation and the coronal plane translations were left unconstrained.

Following AP laxity testing, the knees were positioned for tensile failure testing. The joint capsule, menisci, collateral ligaments, and the posterior cruciate ligament (PCL) were dissected from the joint, leaving the ACL scar mass intact. The tibia and femur were positioned so that the mechanical axis of the ACL was collinear with the load axis of the material test system. The knee flexion angle was initially set at 30°. The tibia was mounted to the base of the material testing machine via a sliding X-Y platform. The femur was unconstrained to rotation. This enabled the specimen to seek its own position so that the load was distributed over the cross-section of the healing ligament when the tensile load was applied. Once the specimen had been placed in the jig, a  $-5$  N compression force was applied to the tibiofemoral joint, at which point the displacement was zeroed. A ramp at 20 mm/min was performed, and the load-displacement data were recorded. The load-displacement data were recorded using TestXpert 10 software (Zwick-Roell; Zwick, Ulm, Germany), and the failure load, failure displacement, and linear stiffness were determined.

### Statistical Analysis

GraphPad Prism 5.0f software (GraphPad, San Diego, CA) was used to analyze the data. Results are presented as means  $\pm$  SEM. Data analysis was conducted using a repeated-measures one-way ANOVA or a two-way ANOVA with Tukey's multiple comparison post hoc test. To assess significance,  $p < 0.05$  was considered statistically significant.

### AUTHOR CONTRIBUTIONS

G.P., K.W.F., Z.G., and D.G. contributed to the concept of the study and revised the manuscript. G.P., M.B., and D.G. designed the experiments. M.B., T.J.K., W.T., and P.A. performed large-animal surgical procedures. M.B., D.S., W.T., and J.C.G. performed ultrasound-mediated gene delivery experiments. M.B., D.S., and W.T. extracted knees and soft tissue samples. M.B., D.S., and S.B.D. performed flow cytometry data analysis. S.B.D. performed RT-PCR assays. J.G.S. performed biomechanics testing. M.B. and G.S. performed the statistical analyses. M.B. performed  $\mu\text{CT}$  and the biomechanical data analysis. M.B., G.S., and G.P. wrote the manuscript.

### CONFLICTS OF INTEREST

Z.G., G.P., and D.G. are shareholders in GamlaStem Medical Inc., which did not provide funds for this study. All other authors declare that they have no competing interests.

### ACKNOWLEDGMENTS

We acknowledge funding from California Institute for Regenerative Medicine (CIRM) grant TR4-06713, the Cedars-Sinai Department of Surgery (to D.G.), the NIH (UL1TR000124 to G.P. and R01CA112356 to K.W.F.), and the United States-Israel Binational Science Foundation Prof. Rahamimoff Travel Grants Program for Young Scientists (to M.B.).

### REFERENCES

- Gordon, M.D., and Steiner, M.E. (2004). Anterior cruciate ligament injuries. In *Orthopaedic Knowledge Update Sports Medicine III*, J.G. Garrick, ed. (American Academy of Orthopaedic Surgeons), pp. 169–182.
- Yabroudi, M.A., Björnsson, H., Lynch, A.D., Muller, B., Samuelsson, K., Tarabichi, M., Karlsson, J., Fu, F.H., Harner, C.D., and Irrgang, J.J. (2016). Predictors of revision surgery after primary anterior cruciate ligament reconstruction. *Orthop. J. Sports Med.* 4, 2325967116666039.
- Smith, L., Xia, Y., Galatz, L.M., Genin, G.M., and Thomopoulos, S. (2012). Tissue-engineering strategies for the tendon/ligament-to-bone insertion. *Connect. Tissue Res.* 53, 95–105.
- Atesok, K., Fu, F.H., Wolf, M.R., Ochi, M., Jazrawi, L.M., Doral, M.N., Lubowitz, J.H., and Rodeo, S.A. (2014). Augmentation of tendon-to-bone healing. *J. Bone Joint Surg. Am.* 96, 513–521.
- Hofbauer, M., Valentin, P., Kdolsky, R., Ostermann, R.C., Graf, A., Figl, M., and Aldrian, S. (2010). Rotational and translational laxity after computer-navigated single- and double-bundle anterior cruciate ligament reconstruction. *Knee Surg. Sports Traumatol. Arthrosc.* 18, 1201–1207.
- Ardern, C.L., Webster, K.E., Taylor, N.F., and Feller, J.A. (2011). Return to sport following anterior cruciate ligament reconstruction surgery: a systematic review and meta-analysis of the state of play. *Br. J. Sports Med.* 45, 596–606.
- Bates, N.A., Myer, G.D., Shearn, J.T., and Hewett, T.E. (2015). Anterior cruciate ligament biomechanics during robotic and mechanical simulations of physiologic and clinical motion tasks: a systematic review and meta-analysis. *Clin. Biomech. (Bristol, Avon)* 30, 1–13.

8. Kohno, T., Ishibashi, Y., Tsuda, E., Kusumi, T., Tanaka, M., and Toh, S. (2007). Immunohistochemical demonstration of growth factors at the tendon-bone interface in anterior cruciate ligament reconstruction using a rabbit model. *J. Orthop. Sci.* 12, 67–73.
9. Rodeo, S.A., Arnoczky, S.P., Torzilli, P.A., Hidaka, C., and Warren, R.F. (1993). Tendon-healing in a bone tunnel. A biomechanical and histological study in the dog. *J. Bone Joint Surg. Am.* 75, 1795–1803.
10. Anderson, K., Seneviratne, A.M., Izawa, K., Atkinson, B.L., Potter, H.G., and Rodeo, S.A. (2001). Augmentation of tendon healing in an intraarticular bone tunnel with use of a bone growth factor. *Am. J. Sports Med.* 29, 689–698.
11. Magnussen, R.A., Granan, L.P., Dunn, W.R., Amendola, A., Andrich, J.T., Brophy, R., Carey, J.L., Flanigan, D., Huston, L.J., Jones, M., et al. (2010). Cross-cultural comparison of patients undergoing ACL reconstruction in the United States and Norway. *Knee Surg. Sports Traumatol. Arthrosc.* 18, 98–105.
12. Persson, A., Fjeldsgaard, K., Gjertsen, J.E., Kjellsen, A.B., Engebretsen, L., Hole, R.M., and Fevang, J.M. (2014). Increased risk of revision with hamstring tendon grafts compared with patellar tendon grafts after anterior cruciate ligament reconstruction: a study of 12,643 patients from the Norwegian Cruciate Ligament Registry, 2004–2012. *Am. J. Sports Med.* 42, 285–291.
13. Rahr-Wagner, L., Thillemann, T.M., Pedersen, A.B., and Lind, M. (2014). Comparison of hamstring tendon and patellar tendon grafts in anterior cruciate ligament reconstruction in a nationwide population-based cohort study: results from the danish registry of knee ligament reconstruction. *Am. J. Sports Med.* 42, 278–284.
14. Tibor, L., Chan, P.H., Funahashi, T.T., Wyatt, R., Maletis, G.B., and Inacio, M.C. (2016). Surgical technique trends in primary ACL reconstruction from 2007 to 2014. *J. Bone Joint Surg. Am.* 98, 1079–1089.
15. Cordrey, L.J. (1963). A comparative study of fresh autogenous and preserved homogenous tendon grafts in rabbits. *J. Bone Joint Surg. Br.* 45-B, 182–195.
16. Jackson, D.W., Corsetti, J., and Simon, T.M. (1996). Biologic incorporation of allograft anterior cruciate ligament replacements. *Clin. Orthop. Relat. Res.* (324), 126–133.
17. Yasuda, K., Tsujino, J., Ohkoshi, Y., Tanabe, Y., and Kaneda, K. (1995). Graft site morbidity with autogenous semitendinosus and gracilis tendons. *Am. J. Sports Med.* 23, 706–714.
18. Wells, D.J. (2004). Gene therapy progress and prospects: electroporation and other physical methods. *Gene Ther.* 11, 1363–1369.
19. Bez, M., Sheyn, D., Tawackoli, W., Avalos, P., Shapiro, G., Giaconi, J.C., Da, X., David, S.B., Gavrity, J., Awad, H.A., et al. (2017). In situ bone tissue engineering via ultrasound-mediated gene delivery to endogenous progenitor cells in mini-pigs. *Sci. Transl. Med.* 9, eaal3128.
20. Feagin, J.A., Jr., Wills, R.P., Lambert, K.L., Mott, H.W., and Cunningham, R.R. (1997). Anterior cruciate ligament reconstruction. Bone-patella tendon-bone versus semitendinosus anatomic reconstruction. *Clin. Orthop. Relat. Res.* (341), 69–72.
21. Spalazzi, J.P., Dagher, E., Doty, S.B., Guo, X.E., Rodeo, S.A., and Lu, H.H. (2008). In vivo evaluation of a multiphased scaffold designed for orthopaedic interface tissue engineering and soft tissue-to-bone integration. *J. Biomed. Mater. Res. A* 86, 1–12.
22. Beynon, B.D., Johnson, R.J., Naud, S., Fleming, B.C., Abate, J.A., Brattbakk, B., and Nichols, C.E. (2011). Accelerated versus nonaccelerated rehabilitation after anterior cruciate ligament reconstruction: a prospective, randomized, double-blind investigation evaluating knee joint laxity using roentgen stereophotogrammetric analysis. *Am. J. Sports Med.* 39, 2536–2548.
23. Tohyama, H., Beynon, B.D., Johnson, R.J., Renström, P.A., and Arms, S.W. (1996). The effect of anterior cruciate ligament graft elongation at the time of implantation on the biomechanical behavior of the graft and knee. *Am. J. Sports Med.* 24, 608–614.
24. Samitier, G., Marciano, A.I., Alentorn-Geli, E., Cugat, R., Farmer, K.W., and Moser, M.W. (2015). Failure of anterior cruciate ligament reconstruction. *Arch. Bone Jt. Surg.* 3, 220–240.
25. Giron, F., Aglietti, P., Cuomo, P., Mondanelli, N., and Ciardullo, A. (2005). Anterior cruciate ligament reconstruction with double-looped semitendinosus and gracilis tendon graft directly fixed to cortical bone: 5-year results. *Knee Surg. Sports Traumatol. Arthrosc.* 13, 81–91.
26. Rodeo, S.A., Kawamura, S., Ma, C.B., Deng, X.H., Sussman, P.S., Hays, P., and Ying, L. (2007). The effect of osteoclastic activity on tendon-to-bone healing: an experimental study in rabbits. *J. Bone Joint Surg. Am.* 89, 2250–2259.
27. Fauno, P., and Kaalund, S. (2005). Tunnel widening after hamstring anterior cruciate ligament reconstruction is influenced by the type of graft fixation used: a prospective randomized study. *Arthroscopy* 21, 1337–1341.
28. Peyrache, M.D., Djian, P., Christel, P., and Witvoet, J. (1996). Tibial tunnel enlargement after anterior cruciate ligament reconstruction by autogenous bone-patellar tendon-bone graft. *Knee Surg. Sports Traumatol. Arthrosc.* 4, 2–8.
29. Struwer, J., Efe, T., Frangen, T.M., Schwarting, T., Buecking, B., Ruchholtz, S., Schüttler, K.F., and Ziring, E. (2012). Prevalence and influence of tibial tunnel widening after isolated anterior cruciate ligament reconstruction using patella-bone-tendon-bone-graft: long-term follow-up. *Orthop. Rev. (Pavia)* 4, e21.
30. Feller, J.A., and Webster, K.E. (2003). A randomized comparison of patellar tendon and hamstring tendon anterior cruciate ligament reconstruction. *Am. J. Sports Med.* 31, 564–573.
31. Maak, T.G., Voos, J.E., Wickiewicz, T.L., and Warren, R.F. (2010). Tunnel widening in revision anterior cruciate ligament reconstruction. *J. Am. Acad. Orthop. Surg.* 18, 695–706.
32. Martinek, V., Latterman, C., Usas, A., Abramowitch, S., Woo, S.L., Fu, F.H., and Huard, J. (2002). Enhancement of tendon-bone integration of anterior cruciate ligament grafts with bone morphogenetic protein-2 gene transfer: a histological and biomechanical study. *J. Bone Joint Surg. Am.* 84-A, 1123–1131.
33. Wang, C.J., Weng, L.H., Hsu, S.L., Sun, Y.C., Yang, Y.J., Chan, Y.S., and Yang, Y.L. (2010). pCMV-BMP-2-transfected cell-mediated gene therapy in anterior cruciate ligament reconstruction in rabbits. *Arthroscopy* 26, 968–976.
34. Kawakami, Y., Takayama, K., Matsumoto, T., Tang, Y., Wang, B., Mifune, Y., Cummins, J.H., Warth, R.J., Kuroda, R., Kurosaka, M., et al. (2017). Anterior cruciate ligament-derived stem cells transduced with BMP2 accelerate graft-bone integration after ACL reconstruction. *Am. J. Sports Med.* 45, 584–597.
35. Mizrahi, O., Sheyn, D., Tawackoli, W., Kallai, I., Oh, A., Su, S., Da, X., Zarrini, P., Cook-Wiens, G., Gazit, D., and Gazit, Z. (2013). BMP-6 is more efficient in bone formation than BMP-2 when overexpressed in mesenchymal stem cells. *Gene Ther.* 20, 370–377.
36. Lavery, K., Swain, P., Falb, D., and Alaoui-Ismaïli, M.H. (2008). BMP-2/4 and BMP-6/7 differentially utilize cell surface receptors to induce osteoblastic differentiation of human bone marrow-derived mesenchymal stem cells. *J. Biol. Chem.* 283, 20948–20958.
37. Li, J.Z., Li, H., Sasaki, T., Holman, D., Beres, B., Dumont, R.J., Pittman, D.D., Hankins, G.R., and Helm, G.A. (2003). Osteogenic potential of five different recombinant human bone morphogenetic protein adenoviral vectors in the rat. *Gene Ther.* 10, 1735–1743.
38. Jane, J.A., Jr., Dunford, B.A., Kron, A., Pittman, D.D., Sasaki, T., Li, J.Z., Li, H., Alden, T.D., Dayoub, H., Hankins, G.R., et al. (2002). Ectopic osteogenesis using adenoviral bone morphogenetic protein (BMP)-4 and BMP-6 gene transfer. *Mol. Ther.* 6, 464–470.
39. Gazit, D., Turgeman, G., Kelley, P., Wang, E., Jalenak, M., Zilberman, Y., and Moutsatsos, I. (1999). Engineered pluripotent mesenchymal cells integrate and differentiate in regenerating bone: a novel cell-mediated gene therapy. *J. Gene Med.* 1, 121–133.
40. Moutsatsos, I.K., Turgeman, G., Zhou, S., Kurkalli, B.G., Pelled, G., Tzur, L., Kelley, P., Stumm, N., Mi, S., Müller, R., et al. (2001). Exogenously regulated stem cell-mediated gene therapy for bone regeneration. *Mol. Ther.* 3, 449–461.
41. Fleming, B.C., Magarian, E.M., Harrison, S.L., Paller, D.J., and Murray, M.M. (2010). Collagen scaffold supplementation does not improve the functional properties of the repaired anterior cruciate ligament. *J. Orthop. Res.* 28, 703–709.
42. Lu, Q.L., Liang, H.D., Partridge, T., and Blomley, M.J. (2003). Microbubble ultrasound improves the efficiency of gene transduction in skeletal muscle in vivo with reduced tissue damage. *Gene Ther.* 10, 396–405.
43. Sheyn, D., Kallai, I., Tawackoli, W., Cohn Yakubovich, D., Oh, A., Su, S., Da, X., Lavi, A., Kimelman-Bleich, N., Zilberman, Y., et al. (2011). Gene-modified adult stem cells regenerate vertebral bone defect in a rat model. *Mol. Pharm.* 8, 1592–1601.

44. Hirpara, K.M., Abouazza, O.A., O'Neill, B., and O'Sullivan, M. (2006). A technique for porcine flexor tendon harvest. *J. Musculoskelet. Res.* 10, 181.
45. Sheyn, D., Shapiro, G., Tawackoli, W., Jun, D.S., Koh, Y., Kang, K.B., Su, S., Da, X., Ben-David, S., Bez, M., et al. (2016). PTH induces systemically administered mesenchymal stem cells to migrate to and regenerate spine injuries. *Mol. Ther.* 24, 318–330.
46. Sheyn, D., Pelled, G., Zilberman, Y., Talasazan, F., Frank, J.M., Gazit, D., and Gazit, Z. (2008). Nonvirally engineered porcine adipose tissue-derived stem cells: use in posterior spinal fusion. *Stem Cells* 26, 1056–1064.
47. Turgeman, G., Pittman, D.D., Müller, R., Kurkalli, B.G., Zhou, S., Pelled, G., Peyser, A., Zilberman, Y., Moutsatsos, I.K., and Gazit, D. (2001). Engineered human mesenchymal stem cells: a novel platform for skeletal cell mediated gene therapy. *J. Gene Med.* 3, 240–251.
48. Murray, M.M., Palmer, M., Abreu, E., Spindler, K.P., Zurakowski, D., and Fleming, B.C. (2009). Platelet-rich plasma alone is not sufficient to enhance suture repair of the ACL in skeletally immature animals: an in vivo study. *J. Orthop. Res.* 27, 639–645.
49. Murray, M.M., Magarian, E., Zurakowski, D., and Fleming, B.C. (2010). Bone-to-bone fixation enhances functional healing of the porcine anterior cruciate ligament using a collagen-platelet composite. *Arthroscopy* 26 (9, Suppl), S49–S57.